Atmospheric
Chemistry
and Physics
Discussions

Secondary organic aerosol formation from primary aliphatic amines with NO$_3$ radical

Q. G. J. Malloy[1,2]**, Li Qi**[1,2]**, B. Warren**[1,2]**, D. R. Cocker III**[1,2]**, M. E. Erupe**[3]**, and P. J. Silva**[3]

[1]University of California-Riverside, Bourns College of Engineering, Department of Chemical and Environmental Engineering, Riverside, California 92521-0001, USA
[2]Bourns College of Engineering, Center for Environmental Research and Technology (CE-CERT), USA
[3]Department of Chemistry and Biochemistry, Utah State University, 0300 Old Main Hall, Logan Utah 84322-0300, USA

Abstract

Primary aliphatic amines are an important class of nitrogen containing compounds found to be emitted from automobiles, waste treatment facilities and agricultural animal operations. A series of experiments conducted at the UC-Riverside/CE-CERT Environmental Chamber is presented in which oxidation of methylamine, ethylamine, propylamine, and butylamine with NO$_3$ has been investigated. Very little aerosol formation is observed in the presence of O$_3$ only. However, after addition of NO, and by extension NO$_3$, large yields of aerosol mass loadings ($\sim$44% for butylamine) are seen. Aerosol generated was determined to be organic in nature due to the small fraction of NO and NO$_2$ in the total signal (<17% for all amines tested) as detected by an aerosol mass spectrometer (AMS). We propose a reaction mechanism between carbonyl containing species and the parent amine leading to formation of particulate imine products. These findings can have significant impacts on rural communities and lead to elevated nighttime PM loadings, when significant levels on NO$_3$ exist.

1 Introduction

Amines are found to be emitted into the atmosphere by a variety of anthropogenic and biogenic sources including automobile emissions, waste treatment facilities, and agricultural animal operations (Westerholm et al., 1993; Manahan, 1990; Schade and Crutzen, 1995). Amine emission rates from dairy operations have been estimated to range from 0.2 to 11 lbs per head of cattle per year (Bailey et al., 2005) additionally, Mosier et al. (1973) has identified cattle feedlots as a major source of methylamine, ethylamine, propylamine, and butylamine as well as other amine compounds.

Removal routes for amines from the atmosphere include reactions with either nitric or sulfuric acid to form the corresponding ammonium salts or oxidation by OH, O$_3$, and NO$_3$ (Seinfeld and Pandis, 1998; Finlayson-Pitts and Pitts, 2000; Silva et al., 2008). The initial step in OH initiated oxidation of aliphatic amines is thought to proceed by four

possible routes (Fig. 1) (Angelino et al., 2001; Schade and Crutzen, 1995). The most predominant route occurs by abstraction of the alpha hydrogen, forming the alkoxy radical after addition of molecular oxygen and NO to NO_2 conversion. The alkoxy radical then proceeds to form an amide. The second route proceeds by loss of an alkyl group from the nitrogen, followed by formation of nitramine, nitrosamine, or imines. Imine's are then believed to undergo reactions leading to formation aldehyde products. It is possible for these oxidation products to be of low enough vapor pressure to condense onto existing particles or form new particles by nucleating, creating secondary organic aerosol (SOA). Once in the aerosol, they can undergo further reactions forming multifunctional species (Pitts et al., 1978).

The presence of organic nitrogen in the particle phase has been reported as far back as the early 1970's when Novakov et al. (1972) found nitrogen with oxidation states similar to that of organic nitrogen compounds in aerosol collected in Pasadena, California. More recently, studies have reported the presence of amine like compounds in ambient particles in both urban and rural settings (Murphy and Thomson, 1997; Angelino et al., 2001; Tan et al., 2002; Glagolenko and Phares, 2004; Beddows et al., 2004). Furthermore, amine like compounds have also been reported in fog water and rain drops obtained in the central valley of California by Zhang and Anastasio (2003).

Recent work has attempted to shed light on the processes that lead to the presence of amines in aerosol through mass spectrometry studies of aerosol generated in smog chambers. These studies have shown that most particles generated from amines are in the form of alkyl ammonium salts with very little organic aerosol formation being seen with the exception of tertiary amines (Angelino et al., 2001; Murphy et al., 2007). Recently, Silva et al. (2008) investigated the reaction of trimethylamine with NO_3 observing the presence of highly oxidized large molecular weight fragments, indicating that the role of NO_3 in amine oxidation warrants further study (Silva et al., 2008).

2 Experimental

All experiments were conducted at the UCR/CE-CERT Environmental Chamber which has been described in detail elsewhere (Carter et al., 2005). In short, this facility consists of two $90\,m^3$ Teflon reactors attached to a rigid collapsible frame, which are maintained at a slight positive pressure to minimize diffusion of any contaminate into the reactors. The reactors are located in a temperature controlled room which is continually flushed with pure air. Connected to the reactors are a suite of instrumentation including an Aerodyne high resolution time of flight mass spectrometer (HR-ToF-AMS), and two scanning mobility particle spectrometers (SMPS), built in house, capable of sizing particles from 30–700 nm (Wang and Flagan, 1990). Particle number and volume were wall loss corrected using the method of Bowman et al. (1997); additionally, particle mass loadings were calculated assuming a unit density. Ports into the chamber enable introduction of compounds of interest as well as monitoring of NO_x using a Thermal Environmental Instruments model 42C chemiluminescent analyzer and O_3 by a Dasibi Environemtal Corp 1003-AH.

Amines were introduced into the chamber by injecting a known volume of liquid amine into a small glass injection manifold or by introducing a known volume of the gas phase amine into a calibrated bulb based on calculated partial pressures. Pure nitrogen was then passed over the liquid or through the bulb, flushing the amine into the reactors. Table 1 lists the experimental conditions of all experiments conducted. 350–400 ppb of ozone was introduced by passing 20 psig of pure air through two UV ozone generators only after immediate particle formation from initial injection of the parent amine had reached a steady state (~2 h). NO_x was added to the reactors as NO using a calibrated bulb approximately 2 h after ozone addition.

Sampling of aerosol for off-line analysis was performed by drawing air from the reactors through a stainless steel sampling port located just below the chamber onto prebaked quartz fiber filters (Pall Life Sciences Laboratory). Filters were then extracted by sonication for 30 min with 5 ml of HPLC grade water (Fisher Scientific Optima Grade).

Extracts were then filtered through a 1 μm pore size syringe filter (Whatman) to remove any quartz fibers and concentrated to 1 ml under a stream of pure nitrogen before analysis.

2.1 High Pressure Liquid Chromatograph – Time Of Flight Mass Spectrometer (HPLC-TOF)

The HPLC-TOF (Agilent Technologies, model 6210) was operated under positive ionization mode with an atmospheric pressure chemical ionization source with a gas temperature of 300°C, vaporizer temperature of 250°C, corona current of 4 μA, drying gas flow of 5 L min^{-1} and a nebulizer pressure of 40 psig. Samples were injected using a flow injection process along with two mass reference compounds to ensure a mass accuracy of 5 ppm or greater.

2.2 High Resolution Time of Flight Aerosol Mass Spectrometer (AMS)

Details of this instrument and data analysis methods has explained in detail by DeCarlo et al. (2006). In brief, the instrument samples through an aerodynamic lens into a time-of-flight chamber; particles between 500–700 nm are transmitted with 100% efficiency. In the time-of-flight chamber particles are accelerated until impacting on to a tungsten heater maintained at 600°C, at which point the non-refractory aerosol vaporizes and is subjected to electron impact ionization at 70 eV.

Ions are guided using a series of lenses to the orthanogonal extractor, ions are pulsed into the time-of-flight chamber approximately every 13 μs. Depending on the mode of operation ions are either reflected towards a mirco-channel plate (MCP) detector following a standard reflectron time-of-flight configuration (V-mode), or ions leaving the reflector are directed first to a hard mirror then back towards the reflector then finally to the MCP (W-mode), more than doubling the path length of V-mode operation.

12699

2.3 Proton Transfer Reaction Mass Spectrometer (PTRMS)

For all experiments conducted, a proton transfer reaction mass spectrometer (Ionicon Analytik) attempted to measure decay of the parent amine. However, in all experiments, no parent amine was detected even though the proton affinity of the amines studied was greater than that of water, which was used in the ionization process. Reasons for the lack of observed signal for the parent amine can be attributed to the difficulty in sampling amine compounds through sampling tubes and the large background interferences for methylamine and ethylamine (Bailey et al., 2005; Shaw et al., 2007).

3 Results and discussion

3.1 Methylamine

Immediate particle formation after methylamine injection resulting from formation of methylammonium nitrate was observed (Fig. 2) followed by volatilization of the salt back into the gas phase. Appearance of particles after addition of NO$_x$ to the chamber was observed; ultimately producing <2 μg/m^3 of aerosol after wall loss correction. Formation of the ammonium salt after addition of NO$_x$ was excluded due to the differences in particle loss rates from those particles observed at the beginning experiment.

Particle composition (Fig. 3) measured by the AMS clearly shows the fragment of *m/z* 30 (NO$^+$/CH$_4$N$^+$), with few higher mass fragments apparent. No addition of NO or NO$_2$ to the amine was seen, ruling out aerosol formation due to nitramines or nitrosamines. Off-line filter analysis was not performed due to the lack of mass formed during the experiment.

3.2 Ethylamine

Particle formation is seen immediately after injection of ethylamine to the reactors (Fig. 4); however, the mass concentration within the reactors remained less than

12700

$1\,\mu g/m^3$ even after addition of ozone. In contrast to methylamine, particle formation increased at a rapid rate once NO was introduced to the chamber, ultimately producing $\sim 80\,\mu g/m^3$.

The mass spectrum as detected by the AMS, normalized to m/z 30, (Fig. 5) shows the m/z fragments appear similar to that of methylamine despite the dramatic differences in aerosol formed, with the exception of the appearance of m/z 44 ($C_2H_6N^+$). However, W-mode data indicates the appearance of a high mass fragments at m/z 59.035 and 100.06 can be attributed to $C_2H_5NO^+$ and $C_4H_8N_2O^+$ respectively, which might account for the variation in aerosol formation.

Filter analysis (Fig. 5) indicates the presence of peaks 88.07605 and 90.09154 which have tentatively been identified as a hydroxyl containing imine ($C_4H_{10}NO^+$) and the stable carbinolamine ($C_4H_{12}NO^+$) respectively. No other peaks of significance are observed, this could be due to the short aliphatic chain of ethylamine.

3.3 Propylamine

Similar to the two previously studied amines, an initial nucleation burst of ammonium salt was apparent immediately after injection of the amine followed by the rapid decay in particle number and volume (Fig. 6). A second rapid burst of particle formation was observed after addition of NO_x to the chamber; similar to the initial burst it was followed by decay of the particle volume indicating possible formation and evaporation of salts. However, the particle mass loading eventually stabilized around $53\,\mu g/m^3$ (after wall loss correction) and very little NO or NO_2 signal was apparent in the high resolution HR-ToF-AMS data, indicating that a large portion of the condensable species formed by the addition of NO_x to the chamber were organic aerosol.

The spectrum obtained by the AMS (Fig. 7) is markedly different from that of methylamine and ethylamine showing prominent mass fragments upwards of m/z 146. Using the W-mode of the AMS these fragments can be attributed to 100.07 ($C_5H_{10}NO^+$), 100.11 ($C_6H_{14}N^+$), 114.09 ($C_6H_{12}NO^+$), 128.11 ($C_6H_{12}N_2O^+$), and

12701

146.08 ($C_6H_{12}NO_3^+$). The appearance of these large fragments, some with no oxygen present, indicates the formation of nitrogen carbon bonds.

Mass spectra, normalized to the highest peak, obtained from the HPLC-TOF (Fig. 7) indicate many peaks that are not apparent in the AMS. The 74.06088 peak can be tentatively attributed to the amide of propylamine. Also indicated in the HPLC-TOF spectra is the presence of masses 88.07601, 90.09061, 102.08960, and 114.09111. These four peaks have been tentatively identified as imines containing a hydroxyl group ($C_4H_{10}NO^+$) and ($C_5H_{12}NO^+$), a carbonyl group ($C_5H_{12}NO^+$), and the stable carbinolamine ($C_4H_{12}NO^+$) respectively. Interestingly, mass 114.09 appears in both the AMS and HPLC-TOF spectra despite the different ionization methods. A possible explanation of this phenomenon could be ion-molecule reactions occurring in the ionization chamber leading to unexpected ion formation. The absence of peaks corresponding to m/z 128 and m/z 146 in the AMS spectra cannot be explained and requires further investigation.

3.4 Butylamine

Not unlike the three previously examined amines, a large initial nucleation burst was observed followed by a rapid decay in particle number after injection of butylamine into the chamber. Addition of ozone resulted in no obvious change in particle number or mass (Fig. 8). Only after addition of NO_x did we observe a rapid increase in particle mass and number ultimately producing $130\,\mu g/m^3$, resembling the aerosol formation trends of ethylamine and propylamine.

Spectra from the AMS (Fig. 9) indicate high mass fragments much like propylamine. Employing the W-mode of the AMS we were able to identify these peaks as 100.07 ($C_5H_{10}NO^+$), 128.10 ($C_7H_{14}NO^+$), 142.12 ($C_8H_{16}NO^+$), 156.12 ($C_8H_{16}N_2O^+$) 158.11 ($C_8H_{16}NO_2^+$), and 174.11 ($C_8H_{16}NO_3^+$).

Figure 9 also shows the spectrum obtained from a filter sample, again many of the same peaks or their analogues observed in the AMS are seen in the HPLC-TOF in-

12702

cluding 102.09151 ($C_5H_{12}NO^+$), 142.12229 ($C_8H_{16}NO^+$), 158.11767 ($C_8H_{16}NO_2^+$), and 174.11122 ($C_8H_{16}NO_3^+$). Masses 74.09705 ($C_4H_{12}N^+$) and 88.07614 ($C_4H_{10}NO^+$) represent the parent amine and amide formed during oxidation, while mass 142.12229 is thought to correspond to the imine formed from the reaction of butanal and butanamide.

Masses 158 and 174 show among the highest degree of oxidation of any peaks observed, requiring the presence of 2 and 3 oxygen molecules respectively. Presumption of a structure of these two peaks is prevented due to multiple possible empirical formulas.

The appearance of masses 142, 158 and 174 in both the AMS and HPLC-TOF spectrums could be due to the same ion-molecule interactions seen with *m/z* 114 in the propylamine/NO$_3$ system. Similar to propylamine, the absence of a peak analogous to the *m/z* 156 peak seen in the AMS needs to further be explored.

3.5 Mass spectrum comparison and proposed aerosol formation mechanism

The presence of an amide peak in all three aerosol forming systems coupled with the lack of its appearance in the methylamine system (Fig. 10) indicates that it could be a major aerosol formation precursor in all three systems. This is further verified from the high resolution of HPLC-TOF, where the presence of the amide peak was confirmed for propylamine and butylamine (the ethylamine amide mass is below the *m/z* capabilities of the HPLC-TOF).

Two trends can be seen from the spectra obtained. The first is the formation of imines which contain a hydroxyl group (mass 88.07605 for ethylamine, mass 114.0911 for propylamine, and mass 142.12229 for butylamine). The second series observed is the presence of imines containing a carbonyl group (100.06 for ethylamine, 128.11 for propylamine, and 156.12 for butylamine). These peaks show extremely large carbon to oxygen ratios and carbon to nitrogen ratios, allowing us to discount aldol condensation reactions as those leading to their formation.

Additionally, using the high resolution capabilities of the AMS, we can exclude the corresponding salts as a significant portion of the aerosol formed due to the small

contribution of NO and NO$_2$ to the total aerosol signal (Fig. 11).

Thus, we propose a reaction sequence (Fig. 12) similar to that of formation of a Schiff base. In this reaction, a carbonyl group generated from loss of an alkyl group from the primary amine or belonging to an amide is protonated and subsequently reacts with the parent amine forming a stable carbinolamine intermediate. The carbinolamine can then undergo unimolecular decomposition followed by loss of the hydrogen from the nitrogen ultimately leading to formation of an imine. This reaction has been observed on particle surfaces, and is known to be promoted in slightly acidic conditions (pH 4–5) (Haddrell and Agnes, 2004; Zahardis et al., 2008; Jencks, 1959). However, without structural information, the assignments of mass spectrum peaks remain tentative and can only be extended to empirical formula confirmation. Therefore, other reaction mechanisms cannot be completely ruled out.

The data presented here indicates that under nighttime conditions, the reaction of primary amines with the nitrate radical can be of great importance. While imine formation appeared to dominate the aerosol mass spectra, other SOA products may have also contributed to the aerosol generated. Therefore, aerosol formation from amines maybe greatly under predicted by current models and further research is needed in order to understand the complex interactions of amines and NO$_3$ in the lower troposphere.

References

Angelino, S., Suess, D. T., and Prather, K. A.: Formation of aerosol particles from reactions of secondary and tertiary alkylamines: Characterization by aerosol time-of-flight mass spectrometry, Environ. Sci. Technol., 35, 3130–3138, 2001.

Bailey, D., Cativiela, J. P., Descary, B., Grantz, D., Hamilton, K. D., Martin, P. E., Meyer, D., Mullinax, D., Simunovic, C. A., Sweet, J., Warner, D., and Watson, J.: San Joaquin Valley Air Pollution Control District, Dairy Emissions Factors for Volatile Organic Compounds, http://www.valleyair.org/busind/pto/dpag/APCO%20Determination%20of%20EF_August%201_.pdf, 2005.

Beddows, D. C. S., Donovan, R. J., Harrison, R. M., Heal, M. R., Kinnersley, R. P., King, M. D., Nicholson, D. H., and Thompson, K. C.: Correlations in the chemical composition of rural background atmospheric aerosol in the UK determined in real time using time-of-flight mass spectrometry, J. Environ. Monitor., 6, 124–133, 2004.

Bowman, F. M., Odum, J. R., Seinfeld, J. H., and Pandis, S. N.: Mathematical model for gas-phase partitioning of secondary organic aerosols, Atmos. Environ., 31, 3921–3931, 1997.

Carter, W. P. L., Cocker, D. R., Fitz, D. R., Malkina, I. L., Bumiller, K., Sauer, C. G., Pisano, J. T., Bufalino, C., and Song, C.: A new environmental chamber for evaluation of gas-phase chemical mechanisms and secondary aerosol formation, Atmos. Environ., 39, 7768–7788, 2005.

Finlayson-Pitts, B. and Pitts, J. N.: Chemistry of the Upper and Lower Atmosphere, Academic Press, 2000.

Glagolenko, S. and Phares, D. J.: Single-particle analysis of ultrafine aerosol in College Station, Texas, J. Geophys. Res.-Atms., 109, D18205, doi:10.1029/2004JD004621, 2004.

Haddrell, A. E. and Agnes, G. R.: A class of heterogeneous/multiphase organic reactions studied on droplets/particles levitated in a laboratory environment: aldehyde plus 1,8-diaminonaphthalene equals imine, Atmos. Environ., 38, 545–556, 2004.

Jencks, W. P.: Studies on the Mechanism of Oxime and Semicarbazone Formation, J. Am. Chem. Soc., 81, 475–481, 1959.

Manahan, S. E.: Environmental Chemistry, 4th Ed., Lewis, 1990.

Mosier, A. R., Andre, C. E., and Viets, F. G.: Identification of Aliphatic-Amines Volatilized from Cattle Feedyard, Environ. Sci. Technol., 7, 642–644, 1973.

Murphy, D. M. and Thomson, D. S.: Chemical composition of single aerosol particles at Idaho

12705

Hill: Positive ion measurements, J. Geophys. Res.-Atms., 102, 6341–6352, 1997.

Murphy, S. M., Sorooshian, A., Kroll, J. H., Ng, N. L., Chhabra, P., Tong, C., Surratt, J. D., Knipping, E., Flagan, R. C., and Seinfeld, J. H.: Secondary aerosol formation from atmospheric reactions of aliphatic amines, Atmos. Chem. Phys., 7, 2313–2337, 2007, http://www.atmos-chem-phys.net/7/2313/2007/.

Novakov, T., Otvos, J. W., Mueller, P. K., and Alcocer, A. E.: Chemical Composition of Pasadena Aerosol by Particle-Size and Time of Day. 3. Chemical States of Nitrogen and Sulfur by Photoelectron Spectroscopy, J. Colloid Interf. Sci., 39, 225–234, 1972.

Pitts, J. N., Grosjean, D., Vancauwenberghe, K., Schmid, J. P., and Fitz, D. R.: Photo-Oxidation of Aliphatic-Amines under Simulated Atmospheric Conditions – Formation of Nitrosamines, Nitramines, Amides, and Photo-Chemical Oxidant, Environ. Sci. Technol., 12, 946–953, 1978.

Schade, G. W. and Crutzen, P. J.: Emission of Aliphatic-Amines from Animal Husbandry and Their Reactions – Potential Source of N_2O and HCN, J. Atmos. Chem., 22, 319–346, 1995.

Seinfeld, J. H. and Pandis, S. N.: Atmospheric Chemistry and Physics: From Air pollution to Climate Change, John Wiley and Sons, Inc., 1998.

Shaw, S. L., Mitloehner, F. M., Jackson, W., Depeters, E. J., Fadel, J. G., Robinson, P. H., Holzinger, R., and Goldstein, A. H.: Volatile organic compound emissions from dairy cows and their waste as measured by proton-transfer-reaction mass spectrometry, Environ. Sci. Technol., 41, 1310–1316, 2007.

Silva, P., Erupe, M., Malloy, Q. G. J., Li, Q., Warren, B., Price, D., Elias, J., and Cocker, D. R.: Trimethylamine as Precursor to Secondary Organic Aerosol Formation via Nitrate Radical Reaction in the Atmosphere, Environ. Sci. Technol., accepted, doi:10.1021/es703016v, 2008.

Tan, P. V., Evans, G. J., Tsai, J., Owega, S., Fila, M. S., and Malpica, O.: On-line analysis of urban particulate matter focusing on elevated wintertime aerosol concentrations, Environ. Sci. Technol., 36, 3512–3518, 2002.

Wang, S. C. and Flagan, R. C.: Scanning Electrical Mobility Spectrometer, Aerosol Sci. Technol., 13, 230–240, 1990.

Westerholm, R., Li, H., and Almen, J.: Estimation of Aliphatic Amine Emissions in Automobile Exhausts, Chemosphere, 27, 1381–1384, 1993.

Zahardis, J., Geddes, S., and Petrucci, G. A.: The ozonolysis of primary aliphatic amines in fine particles, Atmos. Chem. Phys., 8, 1181–1194, 2008,

12706

http://www.atmos-chem-phys.net/8/1181/2008/.

Zhang, Q. and Anastasio, C.: Free and Combined amino compounds in atmospheric fine particles (PM2.5) and for waters from Northern California, Atmos. Environ., 37, 2247–2258, 2003.

12707

Table 1. List of Experiments Performed and Concentrations of reactants.

Experiment	Amine	Estimated Initial Amine Concentration (ppb)	Ozone Concentration (ppb)	NO$_x$ Concentration (ppb)
831	Butylamine	100	352	39
833	Propylamine	100	328	61
834	Methylamine	100	350	34
842	Ethylamine	100	400	25
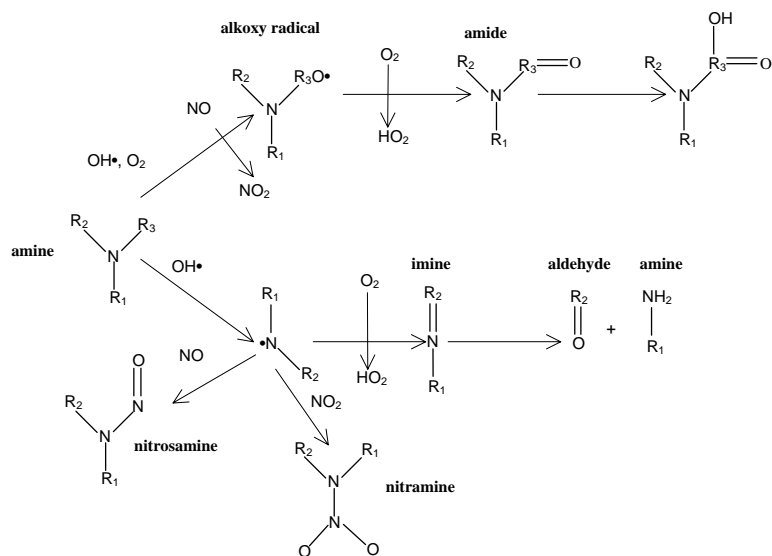
Fig. 1. Reaction mechanism of amines with OH in the presence of NO_x (Schade et al., 1995).
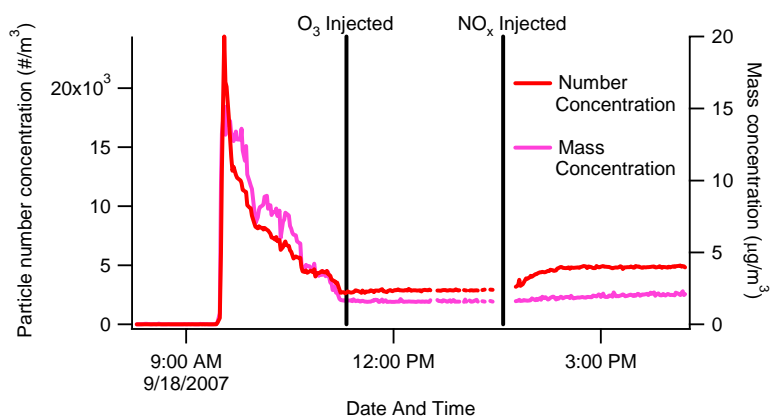
Fig. 2. Wall loss corrected aerosol mass and number evolution for methylamine/$NO_3^\bullet$ reaction showing little organic aerosol formation after addition of NO_x.
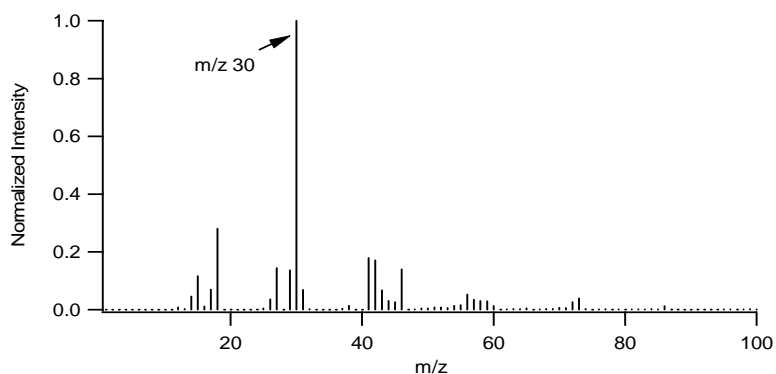
Fig. 3. Background subtracted AMS spectrum normalized to *m/z* 30 from the methylamine/NO$_3^{\bullet}$ system showing no mass fragments other than those of the parent amine.

12711
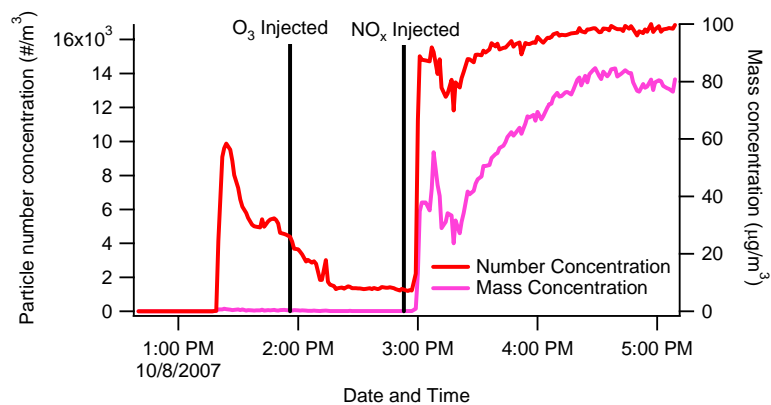
Fig. 4. Wall loss corrected aerosol mass and number evolution for ethylamine/NO$_3^{\bullet}$ reaction indicating a rapid and large increase in organic aerosol formation after addition of NO$_x$.
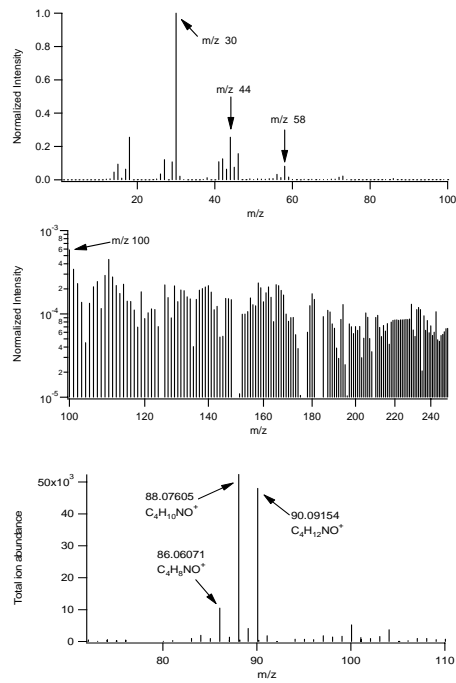
Fig. 5. Frames 1 and 2: AMS mass spectra normalized to *m/z* 30 of the ethylamine/NO$_3^•$ system indicating the important peaks. Frame 3: HPLC-TOF filter spectrum of ethylamine/NO$_3^•$ indicating formation of imines and their stable intermediates.
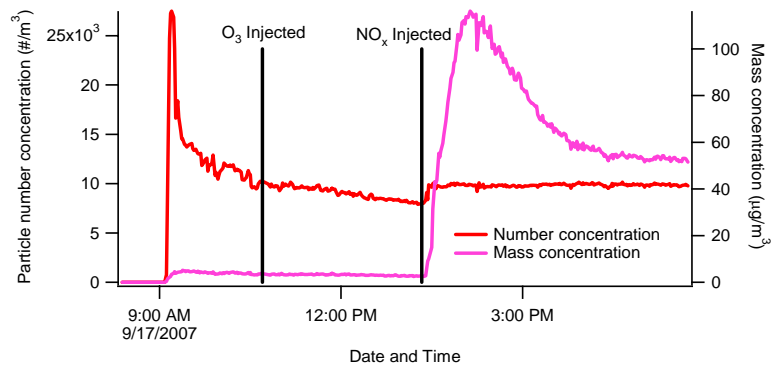
Fig. 6. Wall loss corrected aerosol mass and number evolution for propylamine/NO$_3^•$ reaction indicating a rapid and large increase in aerosol formation after addition of NO$_x$ followed by a rapid loss of a portion of this aerosol.
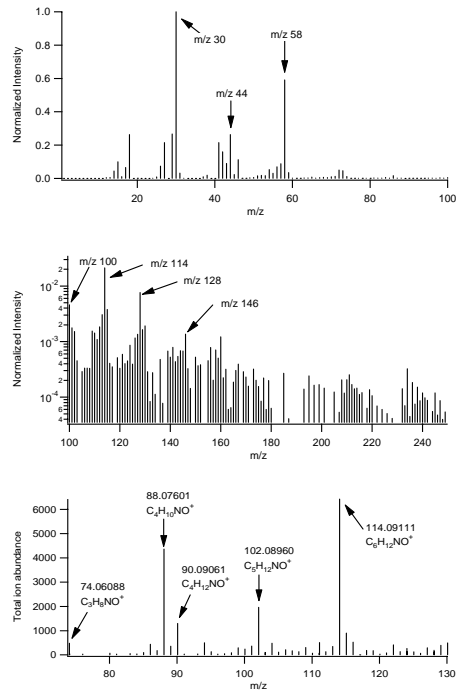
Fig. 7. Frames 1 and 2: AMS spectrum (normalized to *m/z* 30) of the propylamine/ NO$_3^\bullet$ system indicating presence of high mass fragments spaced 14 mass units apart. Frame 3: HPLC-TOF filter spectrum showing imine products and stable intermediates.
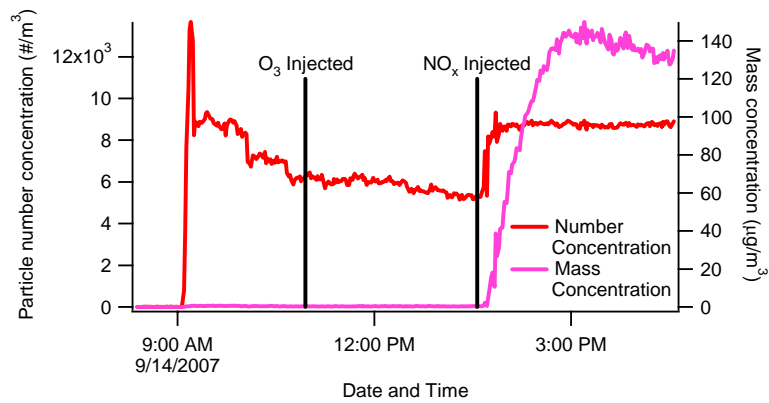
Fig. 8. Wall loss corrected aerosol mass and number evolution for butylamine/NO$_3^\bullet$ reaction indicating a rapid and large increase in organic aerosol formation after addition of NO$_x$.
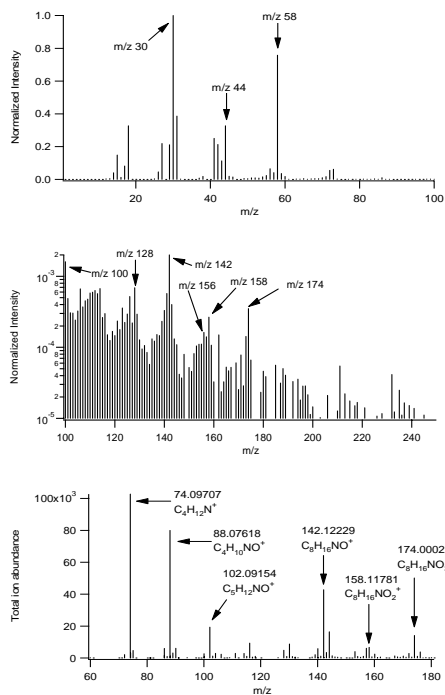
Fig. 9. Frames 1 and 2: AMS spectra normalized to largest peak (*m/z* 30) from butylamine/NO$_3^\bullet$ system showing the formation of imines some with high degrees of oxidation. Frame 3. HPLC-TOF filter spectrum confirming presence of amide products.
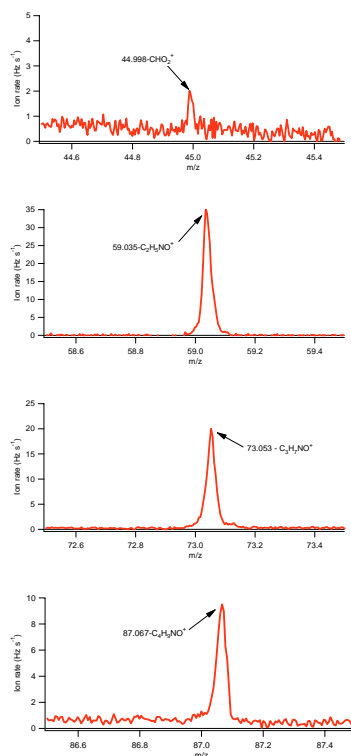
Fig. 10. Background subtracted W-mode spectrums of (from top to bottom) methylamine, ethylamine, propylamine, and butylamine systems indicating amide peaks are only present in the aerosol forming systems.
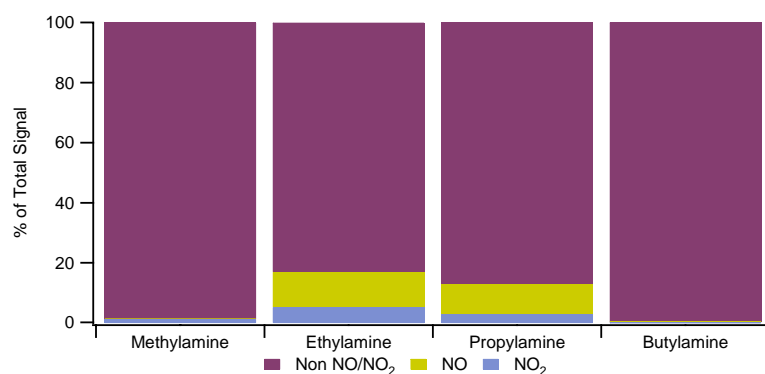
Fig. 11. Contribution of NO and NO$_2$ to the total AMS signal indicating the relative small portion of aerosol that can be attributed to the corresponding ammonium salts.
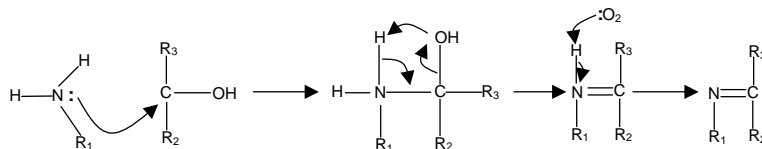
Fig. 12. Proposed reaction mechanism leading to formation of imines (Schiff base) in systems containing primary amines and NO$_3^\bullet$, this reaction is only possible with primary and second amines.